

DMD #52183

**Demonstration of the Innate Electrophilicity of 4-(3-(Benzyloxy)phenyl)-2-(ethylsulfinyl)-6-(trifluoromethyl)pyrimidine (BETP), a Small Molecule Positive Allosteric Modulator of the Glucagon-Like Peptide-1 (GLP-1) Receptor**

Heather Eng, Raman Sharma, Thomas S. McDonald, David J. Edmonds, Jean-Philippe Fortin, Xianping Li, Benjamin D. Stevens, David A. Griffith, Chris Limberakis, Whitney M. Nolte, David A. Price, Margaret Jackson and Amit S. Kalgutkar

*Pharmacokinetics, Dynamics and Metabolism—New Chemical Entities, Groton, CT (H.E., R.S., T.S.M.) and Cambridge, MA (A.S.K.)*

*Cardiovascular, Metabolic and Endocrine Diseases Medicinal Chemistry, Cambridge, MA (D.J.E., B.D.S., D.A.G., W.M.N., D.A.P.) and Groton (C.L.)*

*Cardiovascular, Metabolic and Endocrine Diseases Research Unit, Cambridge, MA (J.P.F., X.L., M.J.)*

*Pfizer, Inc.*

DMD #52183

**Running Title:** Intrinsic electrophilicity of BETP

**Address correspondence to:** Amit S. Kalgutkar, Pharmacokinetics, Dynamics, and Metabolism–New Chemical Entities, Pfizer Worldwide Research and Development, Cambridge, MA 02139. Phone: (617)-551-3336. E-mail: [amit.kalgutkar@pfizer.com](mailto:amit.kalgutkar@pfizer.com)

**Text pages (including references):** 33

**Tables:** 1

**Figures:** 10

**References:** 50

**Abstract:** 245

**Introduction:** 685

**Discussion:** 1038

**Abbreviations used are:** GLP-1, glucagon-like peptide-1; GPCR, G-protein coupled receptor ;  
GLP-1R, glucagon-like peptide-1 receptor; cAMP, cyclic 3'5'-adenosine monophosphate;  
T2DM, type 2 diabetes mellitus; compound B or BETP, 4-(3-(Benzyloxy)phenyl)-2-  
(ethylsulfinyl)-6-(trifluoromethyl)pyrimidine; IVGTT, intravenous glucose tolerance test; i.v.,  
intravenous; p.o., oral; BSA, bovine serum albumin; NADPH, nicotinamide adenine dinucleotide  
phosphate; GSH, glutathione; CDCl<sub>3</sub>, deuterated chloroform; CD<sub>3</sub>OD, deuterated methanol;  
DMSO-*d*<sub>6</sub>, deuterated dimethyl sulfoxide;  $\delta$ , chemical shifts expressed in parts per million; ppm,  
parts per million; s, singlet; d, doublet; t, triplet; q, quartet; m, multiplet; Hz, Hertz; *J*, NMR  
coupling constant in Hertz; *m*CPBA, *meta*-chloroperoxybenzoic acid; LC-MS/MS, liquid  
chromatography tandem mass spectrometry; CYP, cytochrome P450; CHO, Chinese hamster  
ovary; FRET, fluorescence resonance energy transfer; EC<sub>50</sub> half-maximal effective  
concentration; *t*<sub>1/2</sub>, half-life; CID, collision-induced dissociation.

## Abstract

4-(3-(Benzyloxy)phenyl)-2-(ethylsulfinyl)-6-(trifluoromethyl)pyrimidine (BETP) represents a novel small molecule activator of the glucagon-like peptide-1 receptor (GLP-1R), and exhibits glucose-dependent insulin secretion in rats following intravenous (but not oral) administration. In order to explore the quantitative pharmacology associated with GLP-1R agonism in preclinical species, the *in vivo* pharmacokinetics of BETP were examined in rats after intravenous and oral dosing. Failure to detect BETP in circulation after oral administration of a 10 mg/kg dose in rats was consistent with the lack of an insulinotropic effect of orally administered BETP in this species. Likewise, systemic concentrations of BETP in the rat upon intravenous administration (1 mg/kg) were minimal (and sporadic). *In vitro* incubations in bovine serum albumin, plasma and liver microsomes from rodents and human indicated a facile degradation of BETP. Failure to detect metabolites in plasma and liver microsomal incubations in the absence of nicotinamide adenine dinucleotide phosphate was suggestive of a covalent interaction between BETP and a protein amino acid residue(s) in these matrices. Incubations of BETP with glutathione (GSH) in buffer revealed a rapid nucleophilic displacement of the ethylsulfoxide functionality by GSH to yield adduct M1, which indicated that BETP was intrinsically electrophilic. The structure of M1 was unambiguously identified by comparison of its chromatographic and mass spectral properties with an authentic standard. The GSH conjugate of BETP was also characterized in NADPH- and GSH-supplemented liver microsomes, and in plasma samples from the pharmacokinetic studies. Unlike BETP, M1 was inactive as an allosteric modulator of the GLP-1R.

## Introduction

The incretin hormone glucagon-like peptide-1 (GLP-1) is synthesized from proglucagon-derived peptides in intestinal L-cells in response to oral nutrient ingestion (Holst, 2007). The majority of circulating GLP-1 levels comprise the 30-amino acid peptide GLP-1(7-36)NH<sub>2</sub>, which acts through a seven transmembrane-spanning, heterotrimeric class B G-protein coupled receptor (GPCR) on pancreatic  $\beta$  cells to exert glucoregulatory and insulinotropic actions (Thorens, 1992). Binding of GLP-1 to the GLP-1 receptor (GLP-1R) activates the  $G\alpha_s$  subunit, leading to stimulation of membrane-associated adenylyl cyclases and increased production of cyclic 3'5'-adenosine monophosphate (cAMP), which enhances glucose-dependent insulin secretion (Thorens, 1993; Runge et al., 2008). Therapeutic benefits in the treatment of type 2 diabetes mellitus (T2DM) via agonism of the GLP-1R have been demonstrated with the subcutaneously administered agents exenatide in a twice-daily formulation (marketed as Byetta®) or once-weekly formulation (marketed as Bydureon®) and liraglutide in a once-daily formulation (marketed as Victoza®) (Bode, 2011; Murphy, 2012; Jespersen et al., 2013). The efficacies of these agents have been demonstrated in multiple studies, which consistently reported clinically relevant improvements in glycemic control (i.e., reductions in hemoglobin<sub>A1c</sub>, fasting plasma glucose and postprandial plasma glucose excursions) (Madsbad et al. 2011; Scott et al. 2012). Additional injectible GLP-1R agonists (e.g., lixisenatide, dulaglutide and albiglutide) are currently in late stages of clinical development (Madsbad et al. 2011; Meier, 2012).

The success of peptide-based GLP-1R agonists for the treatment of T2DM has also led to discovery efforts aimed at the identification of orally active small molecule agonists of the GLP-1R, which has historically proven to be a difficult task. To a large degree, this difficulty has been

DMD #52183

attributed to the biochemical mechanisms of class B GPCRs, which require large receptor:ligand binding sites to induce signaling. Despite this dilemma, a diverse array of low molecular weight nonpeptidic ligands have been recently reported as antagonists, agonists, and positive allosteric modulators of GLP-1R with intrinsic efficacy (Knudsen et al., 2007; Teng et al., 2007; Sloop et al., 2010; Willard et al., 2012a). 4-(3-(Benzyloxy)phenyl)-2-(ethylsulfinyl)-6-(trifluoromethyl)pyrimidine (compound B or BETP) (Figure 1) is one such analog that has been identified as a positive allosteric modulator of the naturally occurring inactive GLP-1 metabolite, GLP-1(9-36)-NH<sub>2</sub>, while showing little modulation of the active, circulating form i.e., GLP-1(7-36)NH<sub>2</sub> (Sloop et al., 2010; Wootten et al., 2012). Likewise, the insulinotropic effect of oxyntomodulin (glucagon1-37), a low-affinity full agonist of the GLP-1R, was also markedly enhanced in the rat intravenous glucose tolerance test (IVGTT) upon intravenous (i.v.) coadministration with BETP, which is consistent with the *in vitro* biochemical observation of the increased GLP-1R affinity of oxyntomodulin in the presence of BETP (Willard et al., 2012b). *In vivo*, BETP demonstrated glucose-dependent insulin secretion in the IVGTT in rats after i.v. administration. Interestingly, oral (p.o.) administration of BETP failed to show insulinotropic effects similar to those achieved via i.v. administration (Sloop et al., 2010). One possible reason for this discrepancy is that BETP suffers from poor oral absorption due to low aqueous solubility, low absorptive permeability and/or extensive first pass metabolism in the gut and liver.

As part of our general interest in examining quantitative pharmacology for the glucose-dependent insulin secretagogue properties of GLP-1R agonists in preclinical species, the *in vivo* pharmacokinetics of BETP were examined in rats after i.v. and p.o. dosing. To our surprise, little

## DMD #52183

to no systemic exposure of BETP could be measured in plasma samples from both the i.v. and p.o. arms of the pharmacokinetic study. *In vitro* incubations in bovine serum albumin (BSA), plasma and liver microsomes from rodents and human indicated a rapid turnover of BETP. Failure to detect metabolites in BSA, plasma and liver microsomes (in the absence of nicotinamide adenine dinucleotide phosphate (NADPH)) was suggestive of a covalent interaction between BETP and a protein amino acid residue(s) in the various matrices. Consistent with this hypothesis, incubations of BETP with the endogenous antioxidant glutathione (GSH) in buffer revealed a rapid nucleophilic displacement of the ethylsulfoxide functionality by GSH. The GSH conjugate of BETP was also characterized in liver microsomes supplemented with NADPH and GSH, and in plasma samples from the pharmacokinetic studies. The GSH conjugate of BETP was inactive as a positive allosteric modulator of the GLP-1R.

### Materials and Methods

**Materials.** Unless specified otherwise, starting materials used in the synthesis of BETP and its GSH conjugate are generally available from commercial sources such as Aldrich Chemicals Co. (Milwaukee, WI) and Acros Organics (Fairlawn, NJ).  $^1\text{H}$  NMR spectra were recorded in deuterated chloroform ( $\text{CDCl}_3$ ) deuterated methanol ( $\text{CD}_3\text{OD}$ ) or deuterated dimethyl sulfoxide- $d_6$  ( $\text{DMSO}-d_6$ ) on a Varian Unity<sup>TM</sup> 400 MHz spectrometer (DG400-5 probe, available from Varian Inc., Palo Alto, CA) at room temperature. Dimethyl sulfoxide ( $\text{DMSO}-d_6$ ) “100%” was obtained from Cambridge Isotope Laboratories Inc. (Andover, MA). Chemical shifts ( $\delta$ ) are expressed in parts per million (ppm) relative to residual solvent as an internal reference. The peak shapes are denoted as follows: s, singlet; d, doublet; t, triplet; q, quartet; m, multiplet. Coupling constants ( $J$ ) are expressed as Hertz (Hz). GSH, BSA and NADPH were purchased

## DMD #52183

from Sigma-Aldrich (St Louis, MO, USA). Frozen plasma in K<sub>3</sub>EDTA from Wistar-Han rat (pooled males), CD-1 mouse (pooled males) and human (pooled males and females) was purchased from Bioreclamation, Inc. (Westbury, NY, USA). Pooled liver microsomes from human (pool of 50 livers from male/female), male Wistar-Hannover rats, and male CD-1 mice were purchased from BD Biosciences (Woburn, MA). Jugular vein cannulated/ carotid artery cannulated male Wistar-Hannover rats were purchased from Charles River (Raleigh, NC). Solvents used for analysis were of analytical or HPLC grade (Fisher Scientific, Pittsburgh, PA, USA).

**Synthesis of BETP.** A solution of 4-chloro-2-(methylthio)-6-(trifluoromethyl)pyrimidine (**1**, 348 mg, 1.52 mmol), 3-(benzyloxy)phenylboronic acid (**2**, 200 mg, 0.88 mmol) and cesium carbonate (252 mg, 3.88 mmol) in ethylene glycol dimethyl ether (16 ml) and water (4 ml) was degassed with N<sub>2</sub> gas. Tetrakis(triphenylphosphine)palladium(0) (89 mg, 0.08 mmol) was added and the reaction mixture was heated at 85 °C for 18 hours under an N<sub>2</sub> atmosphere. The mixture was then diluted with ethyl acetate (50 ml), dried (sodium sulfate), filtered and concentrated *in vacuo*. The crude product was purified by silica gel chromatography (CombiFlash, 0–3 % ethyl acetate in petroleum ether) to give 4-(3-(benzyloxy)phenyl)-2-(methylthio)-6-(trifluoromethyl)pyrimidine (**3**, 320 mg, 0.85 mmol, 96 %) as a yellow oil. <sup>1</sup>H NMR (400 MHz, CDCl<sub>3</sub>) δ 7.81-7.77 (m, 1 H), 7.69 (d, *J* = 8.0 Hz, 1 H), 7.62 (s, 1 H), 7.54-7.33 (m, 6H), 7.18 (dd, *J* = 2.0, 8.5 Hz, 1 H), 5.18 (s, 2 H), 2.67 (s, 3 H).

To a solution of **3** (340 mg, 0.90 mmol) in dichloromethane (10 ml) was added *meta*-chloroperoxybenzoic acid (*m*CPBA) (468 mg, 2.71mmol) at room temperature. The reaction mixture was stirred at room temperature for 4 hours and then concentrated *in vacuo*. The crude



DMD #52183

product purified by silica gel chromatography (CombiFlash, 0–15 % ethyl acetate in petroleum ether) to give 4-(3-(benzyloxy)phenyl)-2-(methylsulfonyl)-6-(trifluoromethyl)pyrimidine (**4**, 240 mg, 0.59 mmol, 65%) as a yellow oil.  $^1\text{H NMR}$  (400 MHz,  $\text{CDCl}_3$ )  $\delta$  = 8.16 (s, 1H), 7.88 (s, 1 H), 7.79 (d,  $J$  = 7.5 Hz, 1 H), 7.54–7.34 (m, 6 H), 7.25 (br. s., 1H), 5.20 (s, 2 H), 3.47 (s, 3 H).

Compound **4** (1.50 g, 3.67 mmol) was dissolved in tetrahydrofuran (6 ml) and the mixture divided between six microwave reaction tubes. To each tube were added sodium ethanethiolate (154 mg, 1.84 mmol) and ethanethiol (1 ml). The vials were sealed and heated at 100 °C for 20 minutes under microwave irradiation. The six portions were recombined and concentrated, and the crude product was purified by silica gel chromatography (CombiFlash, 0–2 % ethyl acetate in petroleum ether) to give 4-(3-(benzyloxy)phenyl)-2-(ethylthio)-6-(trifluoromethyl)pyrimidine (**5**, 759 mg, 1.95 mmol, 53 %) as a yellow oil.  $m/z$  = 391.0  $[\text{M}+\text{H}]^+$ ;  $^1\text{H NMR}$  (400 MHz,  $\text{CDCl}_3$ )  $\delta$  7.75–7.81 (m, 1H), 7.69 (d,  $J$ =7.53 Hz, 1H), 7.61 (s, 1H), 7.32–7.51 (m, 6H), 7.18 (dd,  $J$ =2.26, 7.78 Hz, 1H), 5.17 (s, 2H), 3.26 (q,  $J$ =7.36 Hz, 2H), 1.47 (t,  $J$ =7.28 Hz, 3H).

To a solution of **5** (700 mg, 1.79 mmol) in dichloromethane (10 ml) was added *m*CPBA (310 mg, 1.79 mmol) portionwise at 0 °C. The reaction mixture was stirred at 0 °C for 30 minutes and quenched by addition of sodium sulfite. The layers were separated and the aqueous portion was extracted with dichloromethane. The combined organic layers were dried over sodium sulfate and concentrated *in vacuo*. The crude product was purified by silica gel chromatography (CombiFlash, 2–24 % ethyl acetate in petroleum ether) to give BETP, 582 mg, 1.43 mmol, 80%) as a white solid.  $m/z$  = 407  $[\text{M}+\text{H}]^+$ ;  $^1\text{H NMR}$  (400 MHz,  $\text{CD}_3\text{OD}$ )  $\delta$  8.49 (s, 1H), 8.08 (s, 1H), 7.97 (d,  $J$ =7.53 Hz, 1H), 7.48–7.58 (m, 3H), 7.37–7.44 (m, 2H), 7.28–7.37 (m, 2H), 5.25 (s, 2H), 3.35–3.47 (m, 1H), 3.19–3.30 (m, 1H), 1.33 (t,  $J$ =7.53 Hz, 3H).

## DMD #52183

**Synthesis of the GSH conjugate of BETP (M1).** To a solution of BETP (100 mg, 0.25 mmol) in a mixture of tetrahydrofuran (2.5 ml) and water (1.0 ml) at room temperature were added GSH (154 mg, 0.50 mmol) and diisopropylethylamine (175  $\mu$ l, 1.0 mmol), and the mixture was stirred for 20 hours at room temperature. The solution was concentrated *in vacuo* and the crude residue was purified by preparative HPLC to afford M1 (165 mg, 0.25 mmol) as a white solid. The preparative HPLC conditions were as follows: HPLC Column: DIKMA Diamonsil(2) C18 5  $\mu$ m, 200 x 20mm. Gradient elution: 30% acetonitrile in water (0.1% trifluoroacetic acid) to 50% acetonitrile in water (0.1% trifluoroacetic acid). The purified product was assessed as >95 % purity by analytical HPLC and  $^1\text{H}$  NMR.  $m/z = 636.0$   $[\text{M}+\text{H}]^+$ ;  $^1\text{H}$  NMR (400 MHz,  $\text{DMSO}-d_6$ )  $\delta$  8.65 (t,  $J=5.52$  Hz, 1H), 8.56 (d,  $J=8.53$  Hz, 1H), 8.30 (s, 1H), 8.01-8.04 (m, 1H), 8.00 (d,  $J=8.03$  Hz, 1H), 7.46-7.54 (m, 3H), 7.37-7.44 (m, 2H), 7.31-7.37 (m, 1H), 7.27 (dd,  $J=2.01$ , 8.03 Hz, 1H), 5.24 (s, 2H), 4.73 (dt,  $J=4.77$ , 8.91 Hz, 1H), 3.96 (dd,  $J=4.52$ , 13.55 Hz, 1H), 3.67-3.80 (m, 2H), 3.55 (t,  $J=6.78$  Hz, 1H), 3.30 (dd,  $J=9.54$ , 13.55 Hz, 1H), 2.34 (t,  $J=7.28$  Hz, 2H), 1.82-2.04 (m, 2H).

**Incubations in Plasma and BSA.** Stock solutions of BETP were prepared in DMSO. BETP (final concentration = 1  $\mu\text{M}$ ) was incubated in 0.1 M potassium phosphate buffer (pH 7.4) supplemented with BSA (10 mg/ml) or in plasma from rat ( $n=3$ ), mouse ( $n=3$ ), and human ( $n=3$ ) at 37  $^\circ\text{C}$  (pH 7.4). Total incubation volume was 0.6 ml and the final DMSO concentration in the incubations was 1% (v/v). Plasmas were thawed and adjusted to pH 7.4. Incubation matrices (594  $\mu$ l) were pre-warmed to 37  $^\circ\text{C}$  and maintained at that temperature for 5 min before adding substrate (6  $\mu$ l). Periodically (0–60 min), aliquots (50  $\mu$ l) of the incubation mixtures were added to acetonitrile (200  $\mu$ l) containing terfenadine (MW = 472, 0.02  $\mu\text{g}/\text{ml}$ ) as an internal standard.

## DMD #52183

Samples were vortexed and then centrifuged at 2300 x *g* for 10 min. Supernatants were analyzed for disappearance of BETP by liquid chromatography tandem mass spectrometry (LC-MS/MS).

**Incubations in Buffer.** BETP (final concentration = 1  $\mu$ M) was incubated in 0.1 M potassium phosphate buffer (pH 7.4) in the absence or presence of GSH (5 mM) at 37 °C (*n*=3). Total incubation volume was 0.6 ml and the final DMSO concentration in the incubations was 5% (v/v). Periodically (0–60 min), aliquots (50  $\mu$ l) of the incubation mixtures were added to acetonitrile (200  $\mu$ l) containing terfenadine (MW = 472, 0.02  $\mu$ g/ml) as an internal standard. Samples were vortexed and then centrifuged at 2300 x *g* for 10 min. Supernatants were analyzed for disappearance of BETP (and concomitant appearance of M1) by LC-MS/MS. The metabolic fate of BETP (10  $\mu$ M) in 0.1 M phosphate buffer (pH 7.4) in the presence of GSH (5 mM) was also examined qualitatively by LC-MS/MS after incubation at 37 °C for 30 min.

**Incubations in Liver Microsomes.** Stock solutions of BETP were prepared in a solution of 1% DMSO and 99% acetonitrile. The final concentrations of DMSO and acetonitrile in the incubation media were 0.01 and 0.99% (v/v), respectively. Microsomal stability assessments were determined in triplicate after incubation of BETP (1  $\mu$ M) with rat, mouse, and human liver microsomes (cytochrome P450 (CYP) concentration, 0.25  $\mu$ M) in 0.1 M potassium phosphate buffer (pH 7.4), containing 3.3 mM magnesium chloride, at 37 °C. Incubations were conducted in the presence or absence of NADPH (1.3 mM) and GSH (5 mM). The total incubation volume was 0.6 ml. Incubations were pre-warmed at 37 °C for 5 min before the addition of BETP. Aliquots (50  $\mu$ l) of the reaction mixture at zero, 2, 5, 10, 20, 40 and 60 min (time period associated with reaction linearity) were added to acetonitrile (200  $\mu$ l) containing terfenadine

## DMD #52183

(MW = 472, 0.02 µg/ml) as an internal standard. The samples were centrifuged at 2300 x g for 10 min before LC-MS/MS analysis for the disappearance of BETP and appearance of M1. For the purposes of qualitative metabolite identification studies, the concentration of BETP in the liver microsomal incubations was raised to 10 µM and that of P450 in rat, mouse, and human liver microsomes was raised to 0.5 µM. After quenching the incubation mixtures with acetonitrile (1 ml), the solutions were centrifuged (2300 x g, 15 min), and the supernatants were dried under a steady nitrogen stream. The residue was reconstituted with the mobile phase and analyzed for metabolite formation by LC-MS/MS.

**Animal Pharmacokinetic Studies.** Rat studies were conducted at Pfizer; all animal care and *in vivo* procedures conducted were in accordance with guidelines of the Pfizer Animal Care and Use Committee. Jugular vein-cannulated male Wistar-Hannover rats (0.25–0.27 kg) were used for pharmacokinetic analysis. For p.o pharmacokinetic studies, animals were fasted overnight before dosing, whereas access to water was provided ad libitum. BETP was administered i.v. via the jugular vein of rats ( $n=2$ ). For p.o. studies, BETP was administered by oral gavage to rats ( $n=2$ ). BETP was administered at 1.0 mg/kg i.v. and 10 mg/kg p.o. Orally dosed rats were fed after collection of the 4-h blood samples. BETP was formulated as a solution in dimethyl sulfoxide-polyethylene glycol 400–water (10:50:40, v/v/v) and 0.5% (w/v) methylcellulose with 2% (v/v) DMSO for the i.v. and p.o. studies, respectively. After dosing, serial plasma samples were collected at appropriate times via the jugular vein cannula and kept frozen at  $-20\text{ }^{\circ}\text{C}$  until LC-MS/MS analysis for presence of BETP and M1

**LC-MS/MS Methodology for Quantification of BETP and M1.** Concentrations of BETP and its GSH adduct (M1) in various matrices (buffer, plasma, and/or liver microsomes) were

## DMD #52183

determined by LC-MS/MS. Briefly, samples/sample extracts were injected by a fixed loop CTC PAL Auto-sampler onto a Shimadzu LC-20AD HPLC system coupled to an AB Sciex API4000 triple quadrupole mass spectrometer fitted with a TurboIonspray source operating in positive ion mode. Chromatographic separation was performed by gradient elution on a Waters HSS T3 XP (30 x 2.1 mm, 2.5  $\mu$ m) reverse phase column, using a binary solvent mixture consisting of 0.1% (v/v) formic acid in water (solvent A) and 0.1% (v/v) formic acid in acetonitrile (solvent B) at a flow rate of 600  $\mu$ l/min. Quantitation was performed by multiple reaction monitoring mode with transitions of 407.2 $\rightarrow$ 379.2 (BETP), 636.2 $\rightarrow$ 507.1 (M1), and 472.2 $\rightarrow$ 436.2 (internal standard: terfenadine). Standards of BETP and M1 in each matrix were fit by least squares regression, and unknown concentrations were determined from the resultant best-fit equation.

**LC-MS/MS Methodology for Metabolite Identification Studies.** Separation of BETP and metabolites was achieved using an ACQUITY UPLC system (Waters Corporation, Milford, USA) with a 2.1  $\times$  150 mm, 1.8  $\mu$ m ACQUITY UPLC HSS C18 column, maintained at a column temperature of 40  $^{\circ}$ C. The mobile phase consisted of water with 0.1% formic acid (A) and acetonitrile (B). The flow rate was 0.3 ml/min and the gradient was as follows: 5% solvent B (0 min), 80% solvent B (5 min) and 5% solvent B (5.2–8.0 min). The injection volume was 15  $\mu$ l. Detection of BETP and metabolites was performed on a SYNAPT G2 (Waters MS Technologies, Manchester, UK) orthogonal acceleration quadrupole time-of-flight mass spectrometry. The MS was operated in positive ion mode using electrospray ionization. The desolvation gas was set to 700 l/h at a temperature of 350  $^{\circ}$ C. The cone gas was set to 30 l/h, and the source temperature to 150  $^{\circ}$ C. The capillary voltage was set to 4 kV, the cone voltage was set to 28V, and the extraction cone to 7V. The SYNAPT G2 was operated in V optics mode (sensitivity mode) with

## DMD #52183

resolution greater than 10,000 at full-width at half-maximum. The data acquisition rate was 0.10 s/scan; data were collected from 1 to 8 min in MS<sup>e</sup> acquisition mode with a collision energy ramp of 25-45V for high energy scans. The MS was calibrated to a mass accuracy under 5 mDa. Data were collected in continuum mode from *m/z* 100 to 900. MassLynx version 4.1, SCN 803 software (Waters Corporation) was used for data processing.

**Cell Culture and cAMP Assay.** Chinese Hamster Ovary (CHO) cells stably expressing the human GLP-1R (CHO-GLP1R cells) were maintained in a DMEM/F-12 Mixture (Invitrogen # 11330032) supplemented with 500 µg/ml G418 (Invitrogen #10131035) and 10% heat-inactivated fetal bovine serum. Cells were grown at 37 °C in a 95% humidified atmosphere consisting of 5% CO<sub>2</sub>. A cell-based time-resolved Fluorescence Resonance Energy Transfer (FRET) assay (Cisbio Bioassays # 62AM4PEJ) was used to measure receptor-mediated cAMP production. This method is based on generation of a FRET signal upon the interaction between (i) an anti-cAMP antibody coupled to a FRET donor (Cryptate) and (ii) a cAMP derivative coupled to a FRET acceptor (d2). Endogenous cAMP produced by cells competes with labeled cAMP for binding to the cAMP antibody, thus reducing the FRET signal. Briefly, CHO-GLP1R cells were dissociated from tissue culture plates using enzyme-free cell dissociation buffer and resuspended in an appropriate volume of assay buffer (1x HBSS (Gibco # 14025-092), 1M HEPES (Gibco # 15630-080)) supplemented with 500µM 3-isobutyl-1-methylxanthine. A total of 2500 cells/well was dispensed into white 384 well plates (BD Falcon # 353988). The metabolite GLP-1(9-36)NH<sub>2</sub> was serially diluted in assay buffer containing BETP (10µM), M1 (10µM) or the corresponding vehicle DMSO. Ligands (5µl of 2 x concentration) were added to the appropriate wells and plates were incubated 30 minutes at room temperature. Five µl of labeled cAMP and 5

## DMD #52183

$\mu\text{l}$  of anti-cAMP antibody were then added to each well and the plates were further incubated at 37 °C for 1 h. Time resolved-FRET signal was measured using an Envision 2103 Multilabel Plate Reader (PerkinElmer) with a laser excitation at 337 nm and dual emissions at 665 nm and 590 nm. A cAMP standard curve diluted in assay buffer was included and used to calculate the amount of cAMP produced, as specified by the manufacturer.

**Data Analysis.** Substrate disappearance half-lives ( $t_{1/2}$ ) were calculated using E-WorkBook 2011 (IDBS, Guildford, Surrey, UK). Sigmoidal curve fitting of ligand concentration-response curves was executed using GraphPad (GraphPad Prism software version 5.02, San Diego, CA). The same software package was used for calculating the half maximal effective concentrations ( $\text{EC}_{50}$  values), an index of ligand potency.

## Results

**Preparation of BETP and its GSH conjugate M1.** BETP was prepared as shown in Figure 1 (panel A). Suzuki coupling (Suzuki, 2005) of chloropyrimidine (**1**) and boronic acid (**2**) derivatives yielded sulfide **3**, which was oxidized with excess mCPBA to yield the corresponding sulfone **4**. Displacement with sodium ethanethiolate introduced the ethyl sulfide (compound **5**), which was oxidized to afford BETP using one equivalent of mCPBA. An authentic sample of M1 was prepared by reacting BETP with GSH in aqueous tetrahydrofuran in the presence of diisopropylethyl amine (Figure 1, panel B).

**Plasma and BSA stability of BETP.** To examine the interspecies stability in plasma, BETP at a concentration of 1  $\mu\text{M}$  was incubated in rat, mouse, and human plasma at 37 °C; periodically, aliquots of the incubation mixture were examined for depletion of BETP. The  $t_{1/2}$  for depletion of

## DMD #52183

BETP in rat, mouse, and human plasma was  $35 \pm 3.0$ ,  $55 \pm 19$ , and  $60 \pm 13$  minutes, respectively. Incubation of BETP ( $1 \mu\text{M}$ ) in potassium phosphate buffer supplemented with  $10 \text{ mg/ml}$  BSA at  $37 \text{ }^\circ\text{C}$  also indicated a decline of the parent compound with a  $t_{1/2}$  of  $54 \pm 5.0 \text{ min}$ .

### **Stability of BETP in potassium phosphate buffer in the presence and absence of GSH.**

BETP ( $1 \mu\text{M}$ ) was stable in phosphate buffer (pH 7.4) at  $37 \text{ }^\circ\text{C}$  ( $t_{1/2} > 120 \text{ min}$ ). However, inclusion of GSH ( $5 \text{ mM}$ ) to the incubation mixture resulted in a rapid disappearance of BETP with a  $t_{1/2}$  of  $< 0.5 \text{ min}$  (Figure 2, panel A). LC-MS/MS analysis of a reaction mixture comprising of BETP ( $10 \mu\text{M}$ ) in potassium phosphate buffer and GSH ( $5 \text{ mM}$ ), incubated at  $37 \text{ }^\circ\text{C}$  for  $30 \text{ min}$ , revealed the formation of a single metabolite denoted as M1 (Figure 3). Under reversed phase HPLC conditions, M1 eluted before BETP (BETP: retention time ( $t_R$ ) =  $6.00 \text{ min}$ ; M1:  $t_R = 4.69 \text{ min}$ ). The collision-induced dissociation (CID) spectra of BETP and M1 are depicted in Figure 4, panels A and B, respectively. M1 displayed a protonated molecular ion ( $\text{MH}^+$ ) at  $m/z$   $636.1734$ , an addition of  $229.0698 \text{ Da}$  to the molecular weight of BETP ( $\text{MH}^+ = 407.1036$ ). The CID spectrum of M1 yielded a diagnostic fragment ion at  $m/z$   $507.1302$ , which corresponds to the neutral loss of the pyroglutamate component in GSH (i.e.,  $129.0426 \text{ Da}$ ), suggesting that M1 was a GSH adduct. Furthermore, the occurrence of the fragment ion at  $m/z$   $363.0772$  is consistent with the presence of an aromatic thioether motif in M1 (Baillie and Davis, 1993). A proposed structure of M1 that is compatible with the observed fragmentation pattern is depicted in Figure 4, panel B. To unambiguously prove the proposed structure, an authentic standard of M1 was synthesized via an independent route. The LC-MS/MS attributes ( $t_R$  and CID spectrum) of the M1 synthetic standard were identical to the one generated in the chemical reaction between BETP and GSH in buffer (data not shown).



## DMD #52183

Based on the qualitative metabolite identification studies, incubations of BETP in GSH-supplemented phosphate buffer were simultaneously monitored for the disappearance of BETP and the appearance of the GSH adduct, respectively (Figure 2, panel B). In phosphate buffer containing GSH, following the 60-min incubation period, the amount of BETP remaining was  $9.0 \pm 1.0$  nM, resulting in a  $492 \pm 40$  nM consumption of BETP when compared with zero minute ( $500 \pm 41$  nM). At 60 min the amount of GSH adduct was  $667 \pm 6.0$  nM, resulting in similar loss of parent substrate BETP and formation of the GSH conjugate.

**Liver microsomal stability of BETP.** To examine liver microsomal stability, BETP at a concentration of 1  $\mu$ M was incubated in rat, mouse, and human liver microsomes at 37 °C for 60 min in the presence and absence of NADPH co-factor, and in the presence and absence of GSH; periodically, aliquots of the incubation mixture were examined for depletion of BETP and the appearance of the GSH adduct of BETP (in liver microsomal incubations supplemented with the thiol nucleophile) (Table 1). The  $t_{1/2}$  for depletion of BETP in rat, mouse, and human liver microsomes in the absence of NADPH and GSH was  $8.8 \pm 0.3$ ,  $5.6 \pm 1.3$ , and  $47 \pm 5.0$  minutes, respectively (Figure 5, panel A). In the presence of NADPH (but absence of GSH), the  $t_{1/2}$  for depletion of BETP in rat, mouse, and human liver microsomes was  $2.2 \pm 0.2$ ,  $0.81 \pm 0.05$ , and  $8.4 \pm 0.3$  min, respectively (Figure 5, panel B). In the presence of both NADPH and GSH, the  $t_{1/2}$  for depletion of BETP in rat, mouse, and human liver microsomes were  $< 0.5$  min.

**Metabolite identification studies.** No metabolites were detected upon qualitative LC-MS/MS examination of incubation mixtures of plasma (rat, mouse and human) and BSA with BETP (10  $\mu$ M) conducted at 37 °C for 60 minutes. Likewise, no metabolite formation was discerned upon incubation of BETP (10  $\mu$ M) with rat, mouse and human liver microsomes in the *absence* of

## DMD #52183

NADPH at 37 °C for 60 minutes. LC-MS/MS analysis of incubation mixtures of BETP (10 μM) with rat, mouse and human liver microsomes in the *presence* of NADPH at 37 °C for 60 minutes revealed the formation of two metabolites (M2 and M3) in each species. A representative chromatogram of a rat liver microsomal incubation with BETP ( $\pm$  NADPH) is shown in Figure 6. The CID spectra of M2 and M3 are depicted in Figure 7, panels A and B, respectively. M2 ( $t_R = 4.54$  min) displayed a  $MH^+$  at  $m/z$  317.0566, which is consistent with *O*-dealkylation in BETP (Figure 7, panel A). M3 ( $t_R = 4.23$  min) displayed a  $MH^+$  at  $m/z$  333.0515, which is consistent with a mono-hydroxylation of M2. A proposed structure for M3 that is compatible with the fragmentation pattern is shown in Figure 7 (panel A). Incubation mixtures of BETP (10 μM) in NADPH- and GSH-supplemented rat, mouse and human liver microsomes revealed the exclusive (and quantitative) conversion to M1 following a 60 minute incubation at 37 °C (data not shown).

**Pharmacokinetic studies in rats.** The *in vivo* formation of M1 was examined in rats after administration of single i.v. (1 mg/kg) and p.o. (10 mg/kg) doses of BETP. Figure 8 illustrates the mean observed plasma concentrations versus time profile of BETP and M1 after i.v. (panel A) or p.o. dosing (panel B). A small quantity ( $\leq 114$  ng/ml, 0.28 μM) of BETP was observed after i.v. dosing, while none was detected after p.o. dosing. The formation of M1 was observed in both dose groups. The rapid appearance of M1 in rat plasma (as early as 1.0 min with peak total plasma concentrations of  $\sim 3.0$  μM) after i.v. dosing indicates the efficiency of the reaction between BETP and GSH in rats. As such, we were unable to estimate pharmacokinetic parameters for BETP due to small and sporadic amounts measureable in the plasma samples.

**Activity of BETP and its GSH conjugate at the human GLP-1R.** Recent work demonstrated that co-incubation with BETP markedly enhances the activity of truncated metabolite of GLP-

## DMD #52183

1(7-36)NH<sub>2</sub> i.e., GLP-1(9-36)NH<sub>2</sub>, at the GLP-1R (Wootten et al., 2012). Here, we took advantage of the latter procedure to test whether the GSH conjugate of BETP (i.e., M1) retains positive allosteric modulator properties of BETP. GLP-1(9-36)NH<sub>2</sub> failed to activate the GLP-1R in the presence of M1 (10 μM) or corresponding DMSO vehicle (Figure 10). In contrast, consistent with previous observations, a dose-dependent increase in cAMP production was observed when CHO-GLP1R cells were stimulated with GLP-1(9-36)-NH<sub>2</sub> in the presence of BETP (10 μM).

### Discussion

Our present studies establish the electrophilic nature of BETP by virtue of its facile chemical reaction with the endogenous nucleophile GSH, which affords the corresponding sulfydryl conjugate M1. A likely mechanism (Figure 10) for the formation of M1 involves nucleophilic attack of GSH on the C2 pyrimidine carbon in BETP to yield the negatively charged  $\sigma$ -complex or Meisenheimer complex followed by elimination of the alkylsulfoxide group as the corresponding sulfenic acid species. The electron-withdrawing substituents (pyrimidine nitrogen atoms in positions 1 and 3 and the trifluoromethyl substituent at position 6) serve to increase the electrophilicity of the C2 carbon via resonance and/or inductive stabilization of the transition state, and favor reaction with the nucleophilic thiol. Certainly, the role of the trifluoromethyl group in accelerating the nucleophilic displacement of 2-halopyridines has been studied (Schlosser and Rausis, 2005). In hindsight, our finding on the innate electrophilicity of BETP is not surprising when one examines the plethora of publications dealing with seemingly “chemically inert” compounds, which are prone to nucleophilic displacement by GSH under non-enzymatic (pH 7.4, phosphate buffer, 37 °C) and/or enzymatic conditions (mediated by

DMD #52183

glutathione transferases in liver microsomes and/or liver cytosol). From a structure-activity relationship perspective, a recurring structural theme in these examples is the presence of the methylsulfone/sulfonamide and/or halide leaving group, which is attached to an electron deficient heteroaromatic ring system (e.g., pyridine, pyridone, benzothiazole, thiadiazole, benzofuran, indole, etc.) (Clapp, 1956; Colucci and Buyske, 1965; Conroy et al., 1984; Graham et al., 1989; Woltersdorf et al., 1989; Graham et al., 1990; Kishida et al., 1990; Huwe et al., 1991; Zhao et al., 1999; Inoue et al., 2009; Litchfield et al., 2010; Teffera et al., 2008). More recently, Yang et al. (2012) have also demonstrated the susceptibility of 2-(alkylthio)-1,3,4-thiadiazoles and 2-(alkylthio)-1,3-benzothiazoles to undergo nucleophilic displacement with GSH in human liver microsomes. The requirement of NADPH co-factor in the GSH displacement reactions suggested that the rate-limiting step involved oxidation of the alkylthio functionality to the corresponding electrophilic sulfoxide and sulfone metabolites, followed by nucleophilic displacement of the formed sulfoxide and/or sulfone by GSH. In the present work, we did not observe further oxidation of the *S*-oxide motif in BETP to the corresponding sulfone metabolite in liver microsomal incubations supplemented with the CYP co-factor NADPH.

Our studies also revealed that BETP was unstable in BSA and plasma from rat, mouse and human, which is contrary to a previous speculation that BETP is stable in plasma (Willard et al., 2012a). Similar to the experience with BSA/plasma, incubations of BETP in rat, mouse and human liver microsomes in the absence of NADPH led to a steady decline in BETP concentrations. Failure to detect products/metabolites in these incubations suggests that the mechanism of BETP depletion proceeds via a covalent displacement reaction between BETP and a nucleophilic amino acid residue(s) in plasma and liver microsomal proteins, similar to the

DMD #52183

pathway depicted with GSH in Figure 10. Inclusion of NADPH and GSH in liver microsomal incubations led to an even more rapid decline of BETP and the quantitative conversion to GSH adduct M1, which is indicative of a detoxifying metabolic pathway that competes with protein covalent binding. The propensity of GSH to reduce microsomal covalent binding has been noted with several drugs that are bioactivated to electrophilic species (Zhao et al., 2007; Obach et al., 2008).

While the protein (plasma/liver microsome) covalent adduction theory has not been proven with a radiolabeled version of BETP, our hypothesis is reasonably supported by literature reports. There are numerous published accounts of covalent interactions between plasma and/or liver microsomal proteins and electrophilic xenobiotics including drugs. Covalent binding of electrophilic acyl glucuronide metabolites has been demonstrated in plasma, notably to albumin, and has been detected *in vivo* in humans for a number of acyl glucuronide-forming drugs (Smith and Wang, 1992; Benet et al., 1993; Ding et al., 1993; Ding et al., 1995; Sallustio et al., 1997). Likewise, covalent modification of lysine residues in human serum albumin has been noted with the electrophilic  $\beta$ -lactam antibiotics such as penicillin G (Levine and Ovary, 1961; Yvon and Wal, 1988; Yvon et al., 1990; Bertucci et al., 2001). Such covalent reactions have also been reported to occur in patients treated with high dosages of  $\beta$ -lactam antibiotics, and are thought to be responsible for the adverse effects associated with this class of compounds (Batchelor et al., 1965; Ahlstedt and Kristofferson, 1982; Lafaye and Lapresle, 1988). Finally, the plasma instability observed with the loop diuretic ethacrynic acid and HKI-272 (an irreversible, covalent inhibitor of tyrosine kinase) have also been attributed to a covalent interaction of their respective  $\alpha,\beta$ -unsaturated carbonyl moieties with amino acid residues in plasma proteins (Bertucci et al.,

DMD #52183

1998; Bertucci and Domenici, 2002; Chandrasekaran et al., 2010; Wang et al., 2010). With respect to covalent binding to liver, both NADPH-dependent and –independent covalent interactions have been demonstrated between liver microsomal proteins and xenobiotics (Evans et al., 2004; Shin et al., 2007).

The failure to detect BETP in circulation following p.o. administration to rats comes as no surprise considering the *in vitro* chemical/biochemical instability of this electrophilic molecule, and the corresponding impact this attribute can have on oral absorption. As such, the lack of an insulinotropic effect of orally administered BETP in the rat IVGTT (Sloop et al., 2010) parallels our inability to detect systemic concentrations of BETP upon administration by the p.o. route. With reference to the glucose-dependent insulin secretion noted over a course of ~ 20 minutes after a single i.v. bolus dose of BETP at 10 mg/kg (Sloop et al., 2010), it is possible that enough BETP systemic exposure was achieved at the i.v. dose of 10 mg/kg to cover the *in vitro* EC<sub>50</sub> of 0.75 μM of BETP against the rat GLP-1R (Sloop et al., 2010). Based on our present work, systemic concentrations of BETP in the rat i.v. pharmacokinetic study at the 1 mg/kg were minimal (and sporadic), but did yield total plasma concentrations of ~ 0.28 μM. The detection of the GSH conjugate M1 at total circulating concentrations significantly higher than BETP in the i.v. pharmacokinetic study (~ 3.0 μM) also led us to examine its role in the positive allosteric modulation of GLP-1R. However, unlike BETP, M1 failed to enhance the activity of GLP-1(9-36)NH<sub>2</sub> at the GLP-1R.

DMD #52183

### **Authorship Contributions**

*Participated in research design:* Kalgutkar, Eng, Sharma, McDonald, Griffith, Stevens, Fortin and Jackson

*Conducted in vitro experiments:* Eng, Sharma, McDonald, Li, Fortin and Nolte

*Contributed new reagents or analytic tools:* Edmonds, Stevens, Griffith, Limberakis and Price

*Performed data analysis:* Kalgutkar, Eng, Sharma, McDonald and Fortin

*Wrote or contributed to the writing of the manuscript:* Kalgutkar, Eng, Sharma, McDonald, Fortin and Griffith

## References

- Ahlstedt S and Kristofferson A (1982) Immune mechanisms for induction of penicillin allergy. *Prog Allergy* **30**:67-134.
- Batchelor FR, Dewdney JM, and Gazzard D (1965) Penicillin allergy: the formation of the penicilloyl determinant. *Nature* **206**:362-364.
- Baillie TA and Davis MR (1993) Mass spectrometry in the analysis of glutathione conjugates. *Biol Mass Spectrom* **22**:319-325.
- Bertucci C, Nanni B, Raffaelli A, and Salvadori P (1998) Chemical modification of human albumin at cys34 by ethacrynic acid: structural characterization and binding properties. *J Pharm Biomed Anal* **18**:127-136.
- Bertucci C, Barsotti MC, Raffaelli A, and Salvadori P (2001) Binding properties of human albumin modified by covalent binding of penicillin. *Biochim Biophys Acta* **1544**:386-392.
- Bertucci C and Domenici E (2002) Reversible and covalent binding of drugs to human serum albumin: methodological approaches and physiological relevance. *Curr Med Chem* **9**:1463-1481.
- Chandrasekaran A, Shen L, Lockhead S, Oganessian A, Wang J, and Scatina J (2010) Reversible covalent binding of neratinib to human serum albumin in vitro. *Drug Metab Lett* **4**:220-227.
- Clapp JW (1956) A new metabolic pathway for a sulfonamide group. *J Biol Chem* **233**:207-214.
- Colucci DF and Buyske DA (1965) The biotransformation of a sulfonamide to a mercaptan and to a mercapturic acid and glucuronide conjugate. *Biochem Pharmacol* **14**:457-466.



DMD #52183

Conroy CW, Schwam H, and Maren TH (1984) The nonenzymatic displacement of the sulfamoyl group from different classes of aromatic compounds by glutathione and cysteine.

*Drug Metab Dispos* **12**:614-618.

Ding A, Ojingwa JC, McDonagh AF, Burlingame AL, and Benet LZ (1993) Evidence for covalent binding of acyl glucuronides to serum albumin via an imine mechanism as revealed by tandem mass spectrometry. *Proc Natl Acad Sci USA* **90**:3797-3801.

Ding A, Zia-Amirhosseini P, McDonagh AF, Burlingame AL, and Benet LZ (1995) Reactivity of tolmetin glucuronide with human serum albumin. Identification of binding sites and mechanisms of reaction by tandem mass spectrometry. *Drug Metab Dispos* **23**:369-376.

Evans DC, Watt AP, Nicoll-Griffith DA, and Baillie TA (2004) Drug-protein adducts: an industry perspective on minimizing the potential for drug bioactivation in drug discovery and development. *Chem Res Toxicol* **17**:3-16.

Graham SL, Shepard KL, Anderson PS, Baldwin JJ, Best DB, Christy ME, Freedman MB, Gautheron P, Habecker CN, Hoffman JM, Lyle PA, Michelson SR, Ponticello GS, Robb CM, Schwam H, Smith AM, Smith RL, Sondey JM, Strohmaier KM, Sugrue MF, and Varga SL (1989) Topically active carbonic anhydrase inhibitors. 2. Benzo[b]thiophenesulfonamide derivatives with ocular hypotensive activity. *J Med Chem* **32**:2548-2554.

Graham SL, Hoffman JM, Gautheron P, Michelson SR, Scholz TH, Schwam H, Shepard KL, Smith AM, Smith RL, Sondey JM, and Sugrue MF (1990) Topically active carbonic anhydrase inhibitors. 3. Benzofuran- and indole-2-sulfonamides. *J Med Chem* **33**:749-754.

- Holst JJ (2007) The physiology of glucagon-like peptide 1. *Physiol Rev* **87**:1409-1439.
- Huwe JK, Feil VJ, Bakke JE, and Mulford DJ (1991) Studies on the displacement of methylthio groups by glutathione. *Xenobiotica* **21**:179-191.
- Inoue K, Ohe T, Mori K, Sagara T, Ishii Y, and Chiba M (2009) Aromatic substitution reaction of 2-chloropyridines catalyzed by microsomal glutathione S-transferase 1. *Drug Metab Dispos* **37**:1797-1800.
- Jespersen MJ, Knop FK, and Christensen M (2013) GLP-1 agonists for type 2 diabetes: pharmacokinetic and toxicological considerations. *Expert Opin Drug Metab Toxicol* **9**:17-29.
- Kishida K, Akaki Y, Sasabe T, Yamamoto C, and Manabe R (1990) Glutathione conjugation of methazolamide and subsequent reactions in the ciliary body in vitro. *J Pharm Sci* **79**:638-642.
- Knudsen LB, Kiel D, Teng M, Behrens C, Bhumralkar D, Kodra JT, Holst JJ, Jeppesen CB, Johnson MD, de Jong JC, Jorgensen AS, Kercher T, Kostrowicki J, Madsen P, Olesen PH, Petersen JS, Poulsen F, Sidelmann UG, Sturis J, Truesdale L, May J, and Lau J (2007) Small molecule agonists for the glucagon-like peptide 1 receptor. *Proc Natl Acad Sci USA* **104**:937-942.
- Lafaye P and Lapresle C (1988) Fixation of penicilloyl groups to albumin and appearance of anti-penicilloyl antibodies in penicillin-treated patients. *J Clin Invest* **82**:7-12.
- Litchfield J, Sharma R, Atkinson K, Filipski KJ, Wright SW, Pfefferkorn JA, Tan B, Kosa RE, Stevens B, Tu M, and Kalgutkar AS (2010) Intrinsic electrophilicity of the 4-methylsulfonyl-2-

pyridone scaffold in glucokinase activators: role of glutathione-S-transferases and in vivo quantitation of a glutathione conjugate in rats. *Bioorg Med Chem Lett* **20**:6262-6267.

Levine BB and Ovary Z (1961) Studies on the mechanism of the formation of the penicillin antigen. III. The *N*-(D- $\alpha$ -benzylpenicilloyl) group as an antigenic determinant responsible for hypersensitivity to penicillin G. *J Exp Med* **144**:875-905.

Madsbad S, Kielgast U, Asmar M, Deacon CF, Torekov SS, and Holst JJ (2011) An overview of once-weekly glucagon-like peptide-1 receptor agonists – available efficacy and safety data and perspectives for the future. *Diabetes Obes Metab* **13**:394-407.

Meier JJ (2012) GLP-1 receptor agonists for individualized treatment of type 2 diabetes mellitus. *Nat Rev Endocrinol* **8**:728-742.

Murphy CE (2012) Review of the safety and efficacy of exenatide once weekly for the treatment of type 2 diabetes mellitus. *Ann Pharmacother* **46**:812-821.

Obach RS, Kalgutkar AS, Soglia JR, and Zhao SX (2008) Can in vitro metabolism-dependent covalent binding data in liver microsomes distinguish hepatotoxic from nonhepatotoxic drugs? An analysis of 18 drugs with consideration of intrinsic clearance and daily dose. *Chem Res Toxicol* **21**:1814-1822.

Runge S, Thøgersen H, Madsen K, Lau J, and Rudolph R (2008) Crystal structure of the ligand-bound glucagon-like peptide-1 receptor extracellular domain. *J Biol Chem* **283**:11340-11347.

Sallustio BC, Fairchild BA, and Pannall PR (1997) Interaction of human serum albumin with the electrophilic metabolite 1-O-gemfibrozil-beta-D-glucuronide. *Drug Metab Dispos* **25**:55-60.

DMD #52183

Schlosser M and Rausis T (2005) The reactivity of 2-fluoro- and 2-chloropyridines toward sodium ethoxide: factors governing the rates of nucleophilic (Het) aromatic substitutions.

*Helvetica Chimica Acta* **88**:1240-1249.

Scott DA, Boye KA, Timlin L, Clark JF, and Best JH (2012) A network meta-analysis to compare glycaemic control in patients with type 2 diabetes treated with exenatide once weekly or liraglutide once daily in comparison with insulin glargine, exenatide twice daily or placebo.

*Diabetes Obes Metab* doi: 10.1111/dom.12007.

Shin NY, Liu Q, Stamer SL, and Liebler DC (2007) Protein targets of reactive electrophiles in human liver microsomes. *Chem Res Toxicol* **20**:859-867.

Sloop KW, Willard FS, Brenner MB, Ficorilli J, Valasek K, Showalter AD, Farb TB, Cao JX, Cox AL, Michael MD, Gutierrez Sanfeliciano SM, Tebbe MJ, and Coghlan MJ (2010) Novel small molecule glucagon-like peptide-1 receptor agonist stimulates insulin secretion in rodents and from human islets. *Diabetes* **59**:3099-3107.

Smith PC and Wang C (1992) Nonenzymic glycation of albumin by acyl glucuronides in vitro. Comparison of reactions with reducing sugars. *Biochem Pharmacol* **44**:1661-1668.

Suzuki A (2005) Carbon-carbon bonding made easy. *Chem Commun (Camb)* **38**:4759-4763.

Tefferia Y, Colletti AE, Harmange JC, Hollis LS, Albrecht BK, Boezio AA, Liu J, and Zhao Z (2008) Chemical reactivity of methoxy 4-o-aryl quinolines: identification of glutathione displacement products in vitro and in vivo. *Chem Res Toxicol* **21**:2216-2222.

DMD #52183

Teng M, Johnson MD, Thomas C, Kiel D, Lakis JN, Kercher T, Aytes S, Kostrowicki J, Bhumralkar D, Truesdale L, May J, Sidelman U, Kodra JT, Jørgensen AS, Olesen PH, de Jong JC, Madsen P, Behrens C, Pettersson I, Knudsen LB, Holst JJ, and Lau J (2007) Small molecule ago-allosteric modulators of the human glucagon-like peptide-1 (hGLP-1) receptor. *Bioorg Med Chem Lett* **17**:5472-5478.

Thorens B (1992) Expression cloning of the pancreatic beta cell receptor for the gluco-incretin hormone glucagon-like peptide 1. *Proc Natl Acad Sci USA* **89**:8641-8645.

Thorens B, Porret A, Bühler L, Deng SP, Morel P, and Widmann C (1993) Cloning and functional expression of the human islet GLP-1 receptor. Demonstration that exendin-4 is an agonist and exendin-(9-39) an antagonist of the receptor. *Diabetes*. **42**:1678-1682.

Wang J, Li-Chan XX, Atherton J, Deng L, Espina R, Yu L, Horwatt P, Ross S, Lockhead S, Ahmad S, Chandrasekaran A, Oganessian A, Scatina J, Mutlib A, and Talaat R (2010) Characterization of HKI-272 covalent binding to human serum albumin. *Drug Metab Dispos* **38**:1083-1093.

Willard FS, Bueno AB, and Sloop KW (2012a) Small molecule drug discovery at the glucagon-like peptide-1 receptor. *Exp Diabetes Res* doi: 10.1155/2012/709893.

Willard FS, Wootten D, Showalter AD, Savage EE, Ficorilli J, Farb TB, Bokvist K, Alsina-Fernandez J, Furness SG, Christopoulos A, Sexton PM, and Sloop KW (2012b) Small molecule allosteric modulation of the glucagon-like Peptide-1 receptor enhances the insulinotropic effect of oxyntomodulin. *Mol Pharmacol* **82**:1066-1073.

DMD #52183

Woltersdorf OW Jr, Schwam H, Bicking JB, Brown SL, deSolms SJ, Fishman DR, Graham SL, Gautheron PD, Hoffman JM, Larson RD, Lee WS, Michelson SR, Robb CM, Share NN, Shepard KL, Smith AM, Smith RL, Sondey JM, Strohmaier KM, Sugrue MF, and Viader MP (1989) Topically active carbonic anhydrase inhibitors. 1. O-acyl derivatives of 6-hydroxybenzothiazole-2-sulfonamide. *J Med Chem* **32**:2486-2492.

Wootten D, Savage EE, Valant C, May LT, Sloop KW, Ficorilli J, Showalter AD, Willard FS, Christopoulos A, and Sexton PM (2012) Allosteric modulation of endogenous metabolites as an avenue for drug discovery. *Mol Pharmacol* **82**:281-290.

Yang Y, Qiu F, Josephs JL, Humphreys WG, and Shu YZ (2012) Bioactivation of 2-(alkylthio)-1,3,4-thiadiazoles and 2-(alkylthio)-1,3-benzothiazoles. *Chem Res Toxicol* **25**:2770-2779.

Yvon M and Wal JM (1988) Identification of lysine residue 199 of human serum albumin as a binding site for benzylpenicilloyl groups. *FEBS Lett* **239**:237-240.

Yvon M, Anglade P, and Wal JM (1990) Identification of the binding sites of benzyl penicilloyl, the allergenic metabolite of penicillin, on the serum albumin molecule. *FEBS Lett* **263**:237-240.

Zhao SX, Dalvie DK, Kelly JM, Soglia JR, Frederick KS, Smith EB, Obach RS, and Kalgutkar AS (2007) NADPH-dependent covalent binding of [3H]paroxetine to human liver microsomes and S-9 fractions: identification of an electrophilic quinone metabolite of paroxetine. *Chem Res Toxicol* **20**:1649-1657.

DMD #52183

Zhao Z, Koeplinger KA, Peterson T, Conradi RA, Burton PS, Suarato A, Henrikson RL, and Tomasselli AG (1999) Mechanism, structure-activity studies, and potential applications of glutathione S-transferase-catalyzed cleavage of sulfonamides. *Drug Metab Dispos* **27**:992-998.

## Figure Legends

Figure 1. Preparation of BETP and its GSH conjugate M1.

Figure 2. (A) Depletion of BETP and (B) appearance of GSH conjugate M1 in incubations of BETP in buffer with and without GSH,  $n=3$ . Mean values and standard deviations are shown.

Figure 3. Extracted ion chromatogram of an incubation mixture of BETP (10  $\mu\text{M}$ ) and GSH (5 mM) in 0.1 M potassium phosphate buffer at 37 °C at  $t = 0$  minutes (panel A) and  $t = 30$  (panel B) minutes.

Figure 4. CID spectrum of BETP (panel A) and GSH conjugate M1 (panel B).

Figure 5. Disappearance of BETP in rat, mouse, and human liver microsomes, in the absence (A) and presence (B) of NADPH (1.3 mM),  $n=3$ . Mean values are plotted and standard deviations are indicated with error bars.

Figure 6. Extracted ion chromatogram of an incubation mixture of BETP (10  $\mu\text{M}$ ) in rat liver microsomes in the absence (panel A) and presence (panel B) of NADPH conducted at 37 °C for 60 minutes.

Figure 7. CID spectra of metabolites M2 (panel A) and M3 (panel B) generated upon incubating BETP (10  $\mu\text{M}$ ) in rat liver microsomes in the presence of NADPH at 37 °C for 60 minutes.

Figure 8. Mean concentration versus time profiles of BETP and its GSH conjugate in rat plasma ( $n=2$ ) after (A) intravenous or (B) oral dosing at 1 mg/kg and 10 mg/kg, respectively. The error bars represent concentration range.



DMD #52183

Figure 9. Allosteric modulation of the human GLP-1R by BETP and the GSH conjugate M1. Ligand stimulated cAMP production was measured in CHO-GLP1R cells. Concentration-response curves are shown for the weak partial agonist GLP-1(9–36)-NH<sub>2</sub> in the presence or BETP, the metabolite M1 or the vehicle DMSO. In contrast to BETP, M1 failed to positively modulate the activity of GLP-1(9–36)-NH<sub>2</sub>. All data represent the mean ± S.E.M. of three independent experiments conducted in quadruplicate.

Figure 10. Nucleophilic displacement of the ethylsulfoxide moiety in BETP by GSH.

DMD #52183

TABLE 1

*In vitro* stability of BETP in liver microsomes (n=3) in the presence and absence of NADPH (1.3 mM) and GSH (5 mM)

Species	NADPH	GSH	$t_{1/2} \pm$ S.D. (min)
Human	-	-	$47 \pm 5.0$
	-	+	$<0.5^a$
	+	-	$8.4 \pm 0.3$
	+	+	$<0.5^a$
Mouse	-	-	$5.6 \pm 1.3$
	-	+	$<0.5^a$
	+	-	$0.81 \pm 0.05$
	+	+	$<0.5^a$
Rat	-	-	$8.8 \pm 0.3$
	-	+	$<0.5^a$
	+	-	$2.2 \pm 0.2$
	+	+	$<0.5^a$

<sup>a</sup> $t_{1/2}$  could not be determined; samples were below the limit of analytical quantitation for BETP at all time points. S.D. = standard deviation.

Figure 1

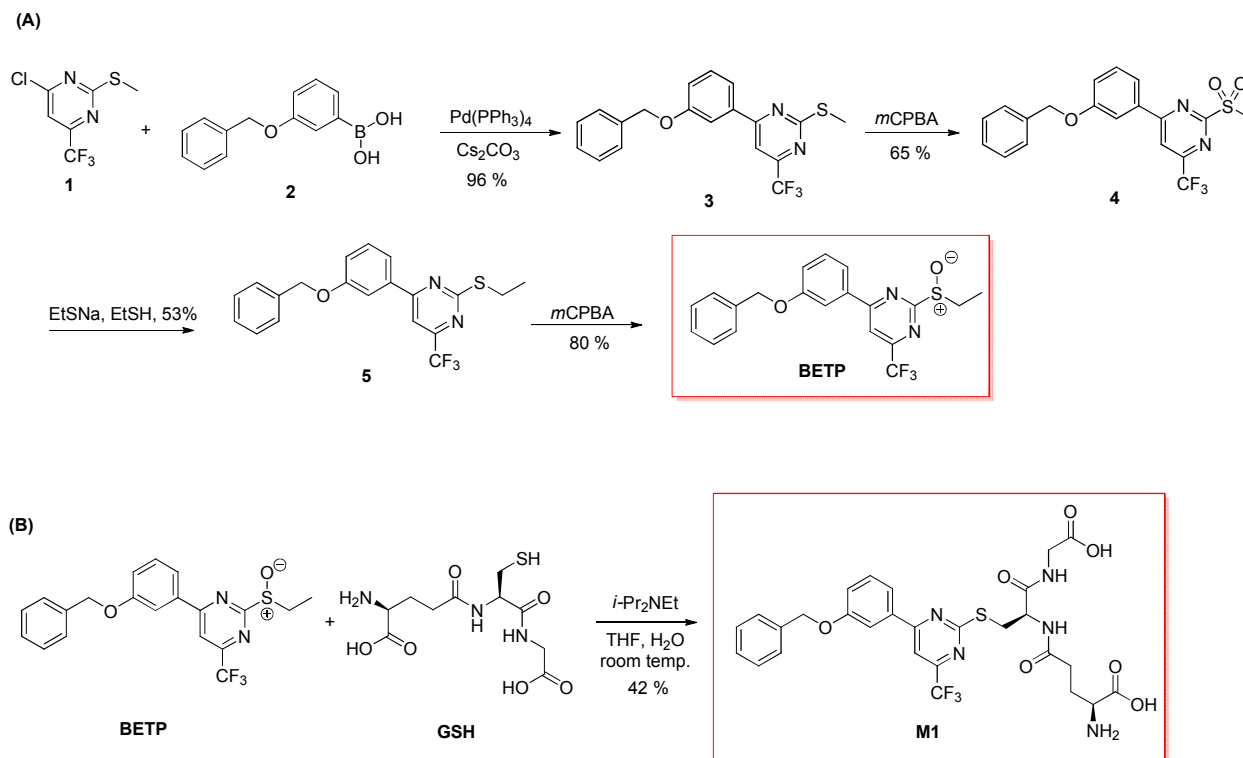
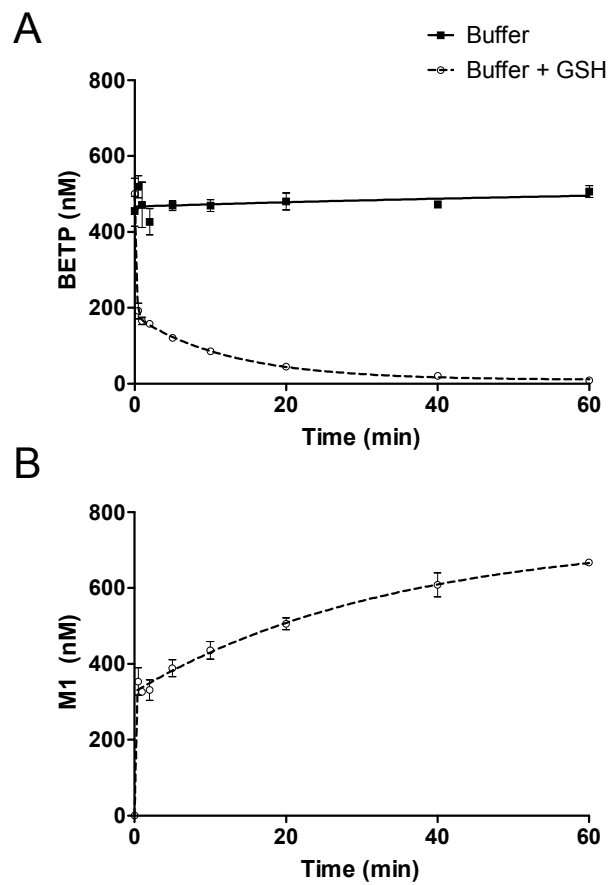
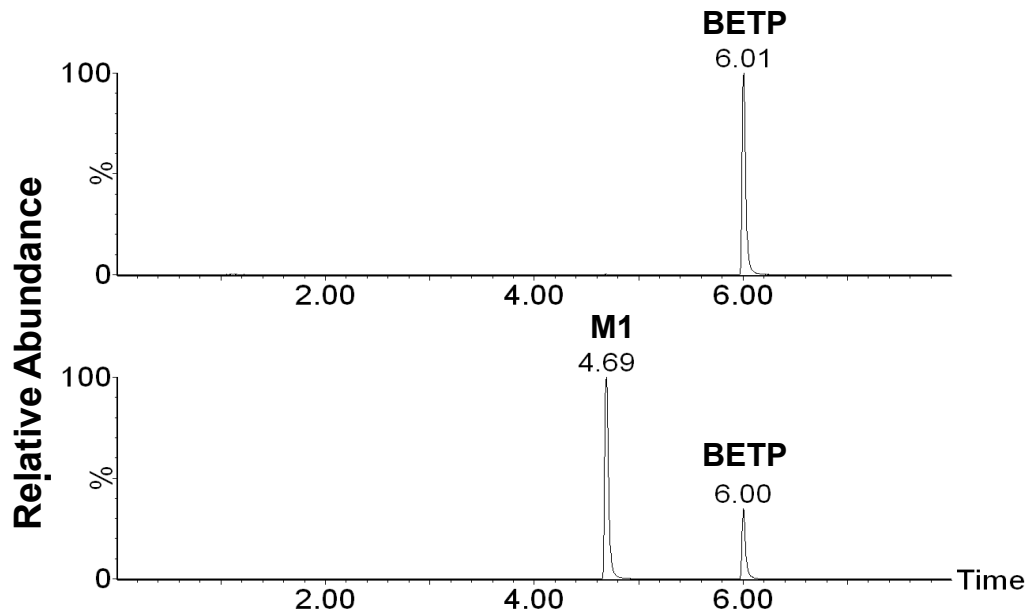


Figure 2





**Figure 3**

Figure 4

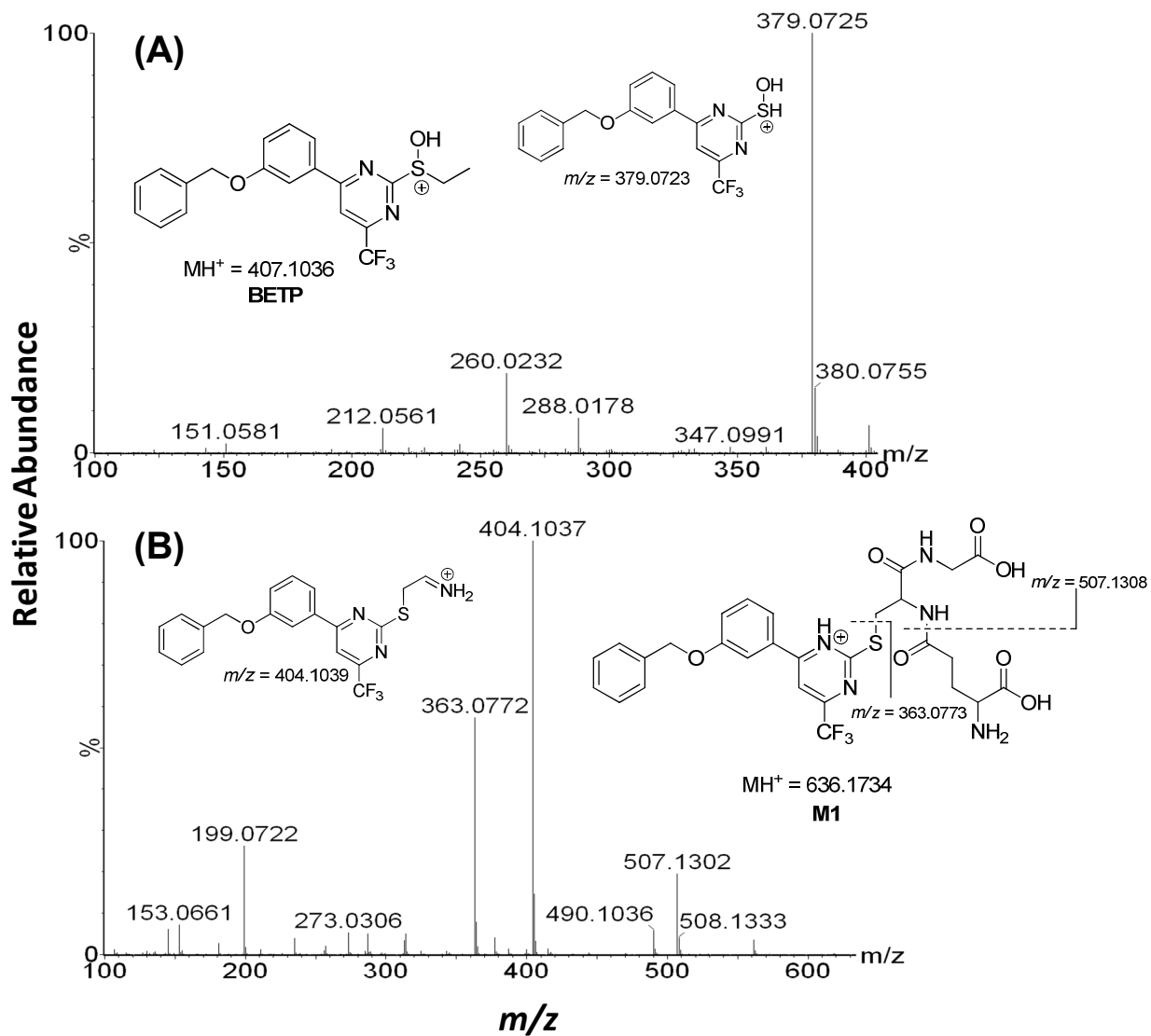
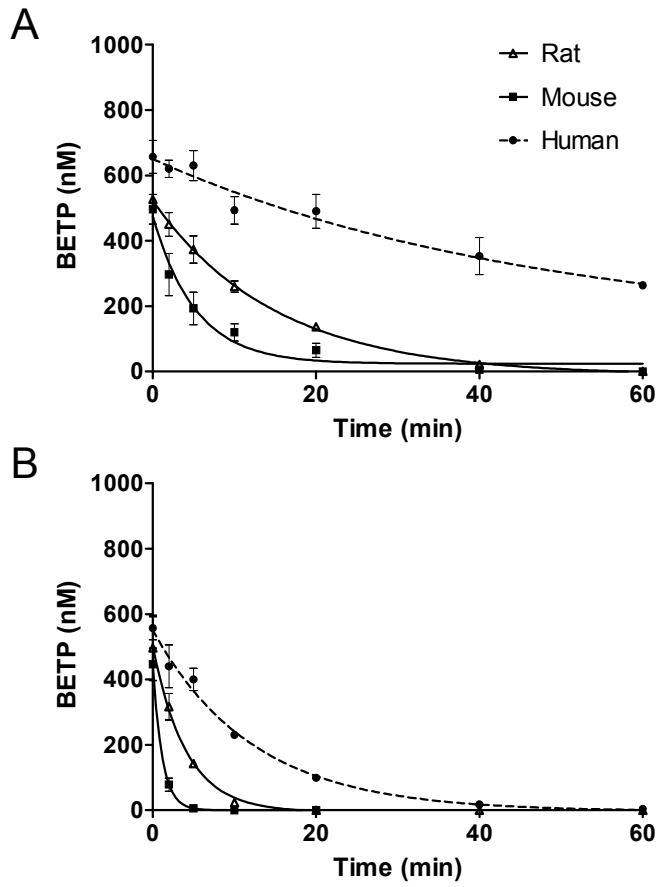


Figure 5



**Figure 6**

Downloaded from dmnd.aspetjournals.org at ASPET Journals on April 20, 2024

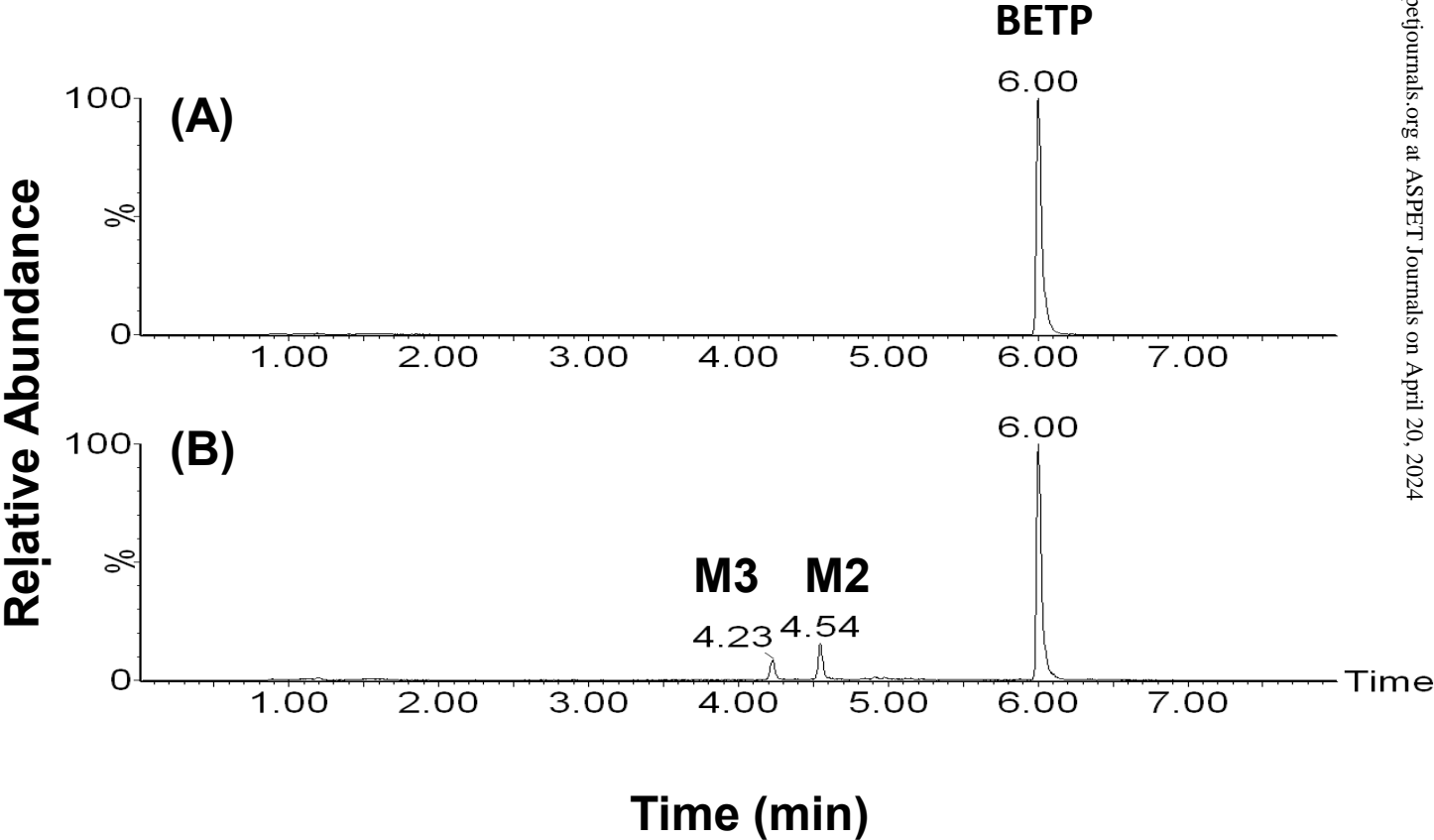




Figure 7

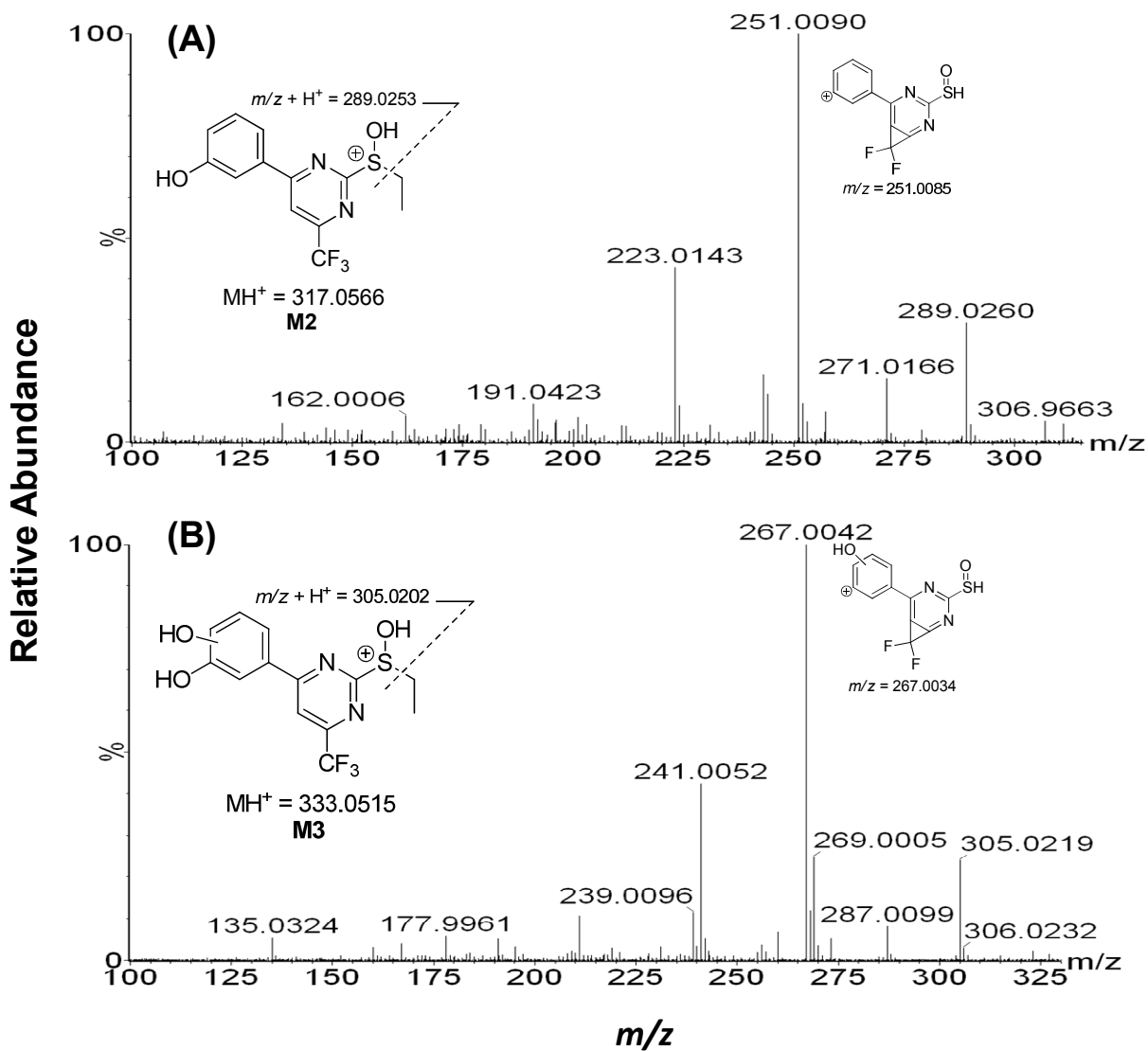


Figure 8

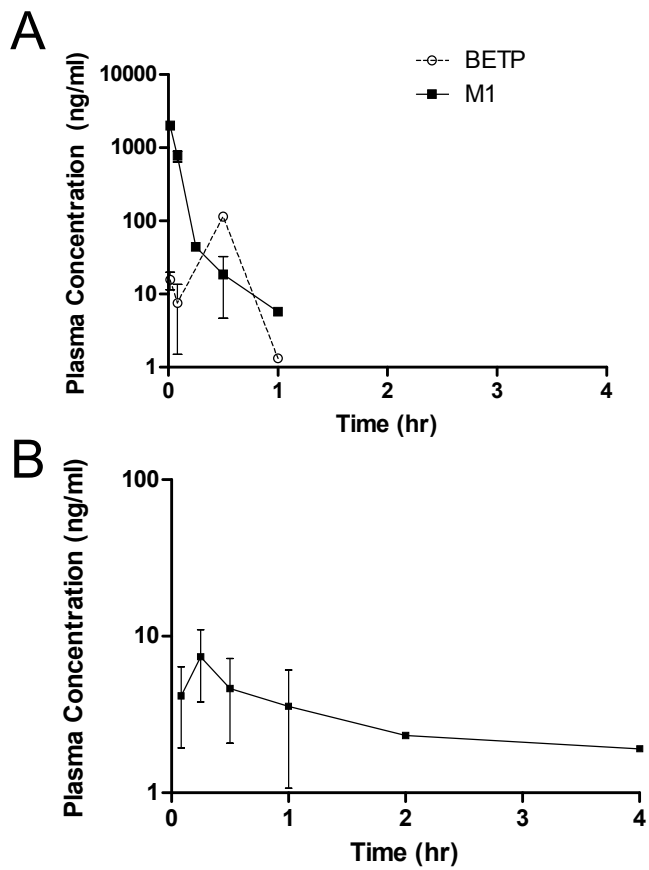
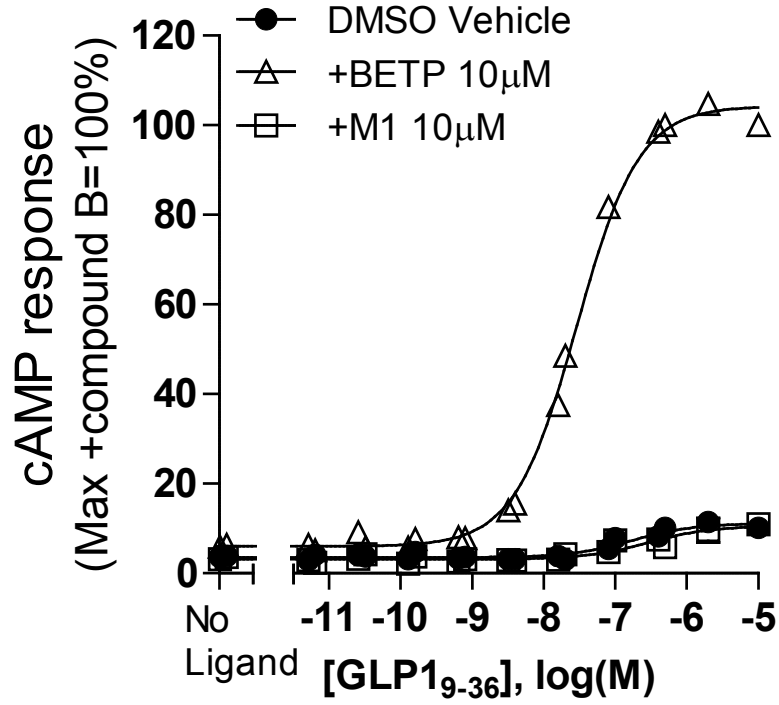


Figure 9



**Figure 10**

